PHILOSOPHICAL TRANSACTIONS OF THE ROYAL SOCIETY A

Phil. Trans. R. Soc. A (2006) **364**, 1683–1708
doi:10.1098/rsta.2006.1795
Published online 25 May 2006

Recent trends in Antarctic snow accumulation from Polar MM5 simulations

By Andrew J. Monaghan[1,2,*], David H. Bromwich[1,2] and Sheng-Hung Wang[1]

[1]*Polar Meteorology Group, Byrd Polar Research Center, and* [2]*Atmospheric Sciences Program, Department of Geography, The Ohio State University, Columbus, 1090 Carmack Road, Columbus, OH 43210, USA*

Polar MM5, a mesoscale atmospheric model optimized for use over polar ice sheets, is employed to simulate Antarctic accumulation in recent decades. Two sets of simulations, each with different initial and boundary conditions, are evaluated for the 17 yr period spanning 1985–2001. The initial and boundary conditions for the two sets of runs are provided by the (i) European Centre for Medium-Range Weather Forecasts 40 year Reanalysis, and (ii) National Centres for Environmental Prediction—Department of Energy Atmospheric Model Intercomparison Project Reanalysis II. This approach is used so that uncertainty can be assessed by comparing the two resulting datasets.

There is broad agreement between the two datasets for the annual precipitation trends for 1985–2001. These generally agree with ice core and snow stake accumulation records at various locations around the continent, indicating broad areas of both upward and downward trends. Averaged over the continent the annual trends are small and not statistically different from zero, suggesting that recent Antarctic snowfall changes do not mitigate current sea-level rise. However, this result does not suggest that Antarctica is isolated from the recent climate changes occurring elsewhere on Earth. Rather, these are expressed by strong seasonal and regional precipitation changes.

Keywords: Antarctic accumulation; Antarctic precipitation; Antarctic surface mass balance

1. Introduction

(*a*) *General spatial and temporal characteristics of Antarctic precipitation*

The accumulation term is the primary mass input to the Antarctic ice sheets, and is the net result of precipitation, sublimation/vapour deposition, drifting snow processes and melt. Precipitation is dominant among these components (Bromwich 1988) and establishing its spatial and temporal variability is necessary to assess ice sheet surface mass balance. Comprehensive studies of precipitation characteristics over Antarctica are given by Bromwich (1988), Turner *et al.* (1999), Genthon & Krinner (2001), Van Lipzig *et al.* (2002) and

* Author for correspondence (monaghan.11@osu.edu).

One contribution of 14 to a Discussion Meeting Issue 'Evolution of the Antarctic Ice Sheet: new understanding and challenges'.

Bromwich *et al.* (2004). Precipitation is influenced to first order by the Antarctic topography. Most of the precipitation falls along the steep coastal margins and is caused by orographic lifting of relatively warm, moist air associated with the many transient, synoptic-scale cyclones that encircle the continent. The influence of synoptic activity decreases inward from the coast, and over the highest, coldest reaches of the continent the primary mode of precipitation is due to cooling of moist air just above the surface-based temperature inversion. This extremely cold air has little capacity to hold moisture, and thus the interior of the East Antarctic ice sheet is a polar desert, with a large area that receives less than 5 cm water equivalent each year (e.g. Vaughan *et al.* 1999; Giovinetto & Zwally 2000).

(*b*) *Long-term Antarctic accumulation estimates*

In recent decades, estimates of precipitation and accumulation over the Antarctic ice sheets have been made by three techniques: surface-based observations, remote sensing and atmospheric modelling. Constructing a reliable dataset of snow accumulation and precipitation measurements over Antarctica for a long time-period from these methods has been difficult for numerous reasons. These include a sparse surface observational network (e.g. Giovinetto & Bentley 1985), difficulties distinguishing between clouds and the Antarctic ice surface in satellite radiances (Xie & Arkin 1998), and incomplete parameterizations of polar cloud microphysics and precipitation in atmospheric models (Guo *et al.* 2003), as well as errors in the large-scale circulation (e.g. Bromwich & Fogt 2004). Considering the limitations of these techniques, it is not surprising that the long-term-averaged continent-wide maps of snow accumulation over Antarctica yield a broad spectrum of results. The long-term estimates from several studies range from 119 (Van de Berg *et al.* in press *a*) to 197 mm yr^{-1} (Ohmura *et al.* 1996) for the grounded ice sheet (GIS; estimates for the conterminous ice sheet, which includes the ice shelves, are generally approx. 10% higher). In general, the studies employing glaciological data are considered the most reliable; the study of Vaughan *et al.* (1999) represents the current best approximation of 149 mm yr^{-1} for the GIS, although a recent study (Van de Berg *et al.* in press *b*) shows evidence that the Vaughan *et al.* (1999) dataset may underestimate coastal accumulation. It is anticipated that advancements in all three techniques will reduce the uncertainties in the future.

(*c*) *Recent trends in Antarctic precipitation*

On average, about 6 mm global sea level equivalent falls as precipitation on Antarctica each year (Budd & Simmonds 1991). Thus, it is important to assess trends in Antarctic precipitation, as even small changes can have considerable impacts on the global sea level budget. Vaughan (2005) notes that the greatest uncertainty in future predictions of sea-level rise lies in the contribution of the Antarctic ice sheet, and considering the disagreement between various estimates of long-term accumulation discussed above, our ability to resolve recent trends has been limited. Bromwich *et al.* (2004) inferred an upward trend of about 1.5 mm yr^{-2} precipitation occurred from 1979 to 1999 from large-scale global models. This suggests that the trend in Antarctic precipitation removes an additional approximately 0.05 mm yr^{-1} from the global ocean. This is an important

effect considering the current rate of sea-level rise of $+2.8 \pm 0.4\,\mathrm{mm\,yr^{-1}}$ (Leuliette *et al.* 2004). Davis *et al.* (2005) suggest a much larger negative contribution to global sea-level rise based on observations of thickening over East Antarctica from satellite altimetry. They suggest that most of this thickening is due to increases in precipitation, and that taken collectively, precipitation over East Antarctica to approximately 81° S mitigates sea-level rise by about $0.12\,\mathrm{mm\,yr^{-1}}$ between 1992 and 2003. This result is surprising considering it suggests a significant increase of precipitation over East Antarctica during one decade. There is little evidence of this magnitude of change in the observational records from ice cores and snow stakes examined in this study. The results of Van de Berg *et al.* (in press *a*) for a similar period, 1980–2001, are in contrast. RACMO2/ANT, an atmospheric mesoscale model, shows a statistically insignificant upward trend about an order of magnitude less than Bromwich *et al.* (2004). This may be partly because the initial and boundary conditions are provided by the recently completed European Centre for Medium-Range Weather Forecasts 40 year Reanalysis (ERA-40), which for the same period shows a downward trend of $-0.42\,\mathrm{mm\,yr^{-2}}$. It is difficult to assess model precipitation trends prior to approximately 1979 due to artificial trends or jumps in model fields related to the change in the volume and type of data available at the onset of the modern satellite era (e.g. Hines *et al.* 2000; Van de Berg *et al.* in press *a*).

(*d*) *Description of the current study*

This study employs Polar MM5 to simulate Antarctic accumulation in recent decades. Polar MM5 is a version of the Pennsylvania State University/National Centre for Atmospheric Research (NCAR) fifth generation mesoscale model (MM5; Grell *et al.* 1994) optimized for the environment of polar ice sheets by the Polar Meteorology Group of the Byrd Polar Research Centre at Ohio State University (Bromwich *et al.* 2001; Cassano *et al.* 2001). The two sets of simulations, each with different initial and boundary conditions, are evaluated for the 17 yr period spanning 1985–2001. The initial and boundary conditions for the two sets of runs are provided, respectively, by (i) ERA-40, and (ii) the National Centres for Environmental Prediction—Department of Energy Atmospheric Model Intercomparison Project Reanalysis II (NCEP-II). This approach is used so that uncertainty can be assessed by comparing the two resulting datasets. If the results from the two sets of simulations are similar, this increases confidence that the trends are robust in regions where long-term observational data are absent.

One motivation for this work is that most existing long-term global reanalyses have been performed with models tuned to provide optimal results for lower latitudes. Therefore, they have traditionally had problems that limit their use for assessing climate trends at high latitudes. A thorough review of the problems associated with the various reanalysis datasets is given by Bromwich & Fogt (2004). Here we endeavour to optimize results over Antarctica by employing a model that has proven good skill over the Antarctic (Guo *et al.* 2003), and by using the most up-to-date topography at a horizontal resolution that exceeds the reanalyses (60 km in Polar MM5 versus approx. 125 km in the highest-resolution reanalysis available). Due to the computational expense, only recently have mesoscale models been used to explore Antarctic precipitation at decadal

time-scales (Van Lipzig *et al.* 2002; Van de Berg *et al.* in press *a*). This is the first time Polar MM5 has been used to do so.

In §2, the model formulation and related datasets are described. In §3, the simulated mean accumulation and trends are compared to observationally based datasets to assess their quality. In §4, the spatial distribution of the temporal trends from 1985 to 2001 is evaluated. In §5, the mean precipitation and accumulation and trends averaged over the whole of Antarctica from our simulations and several other datasets are compared. Conclusions are drawn in §6.

2. Polar MM5 configuration

A full description of the standard MM5 modelling system is given by Grell *et al.* (1994). Bromwich *et al.* (2001) and Cassano *et al.* (2001) give a detailed description of the important changes to MM5 to optimize the model for use over ice sheets as Polar MM5. These include a modified parameterization for the prediction of ice cloud fraction, improved cloud–radiation interactions, an optimized stable boundary layer treatment, improved calculation of heat transfer through snow and ice surfaces and the addition of a fractional sea ice surface type. Guo *et al.* (2003) evaluate Polar MM5 performance over Antarctica for a 1 yr period (1993) for a similar model configuration and show that the intraseasonal and interseasonal variability in pressure, temperature, wind and moisture are well-resolved.

A 60 km polar stereographic domain with 121 grid points in the x and y directions covers Antarctica and the surrounding ocean (figure 1). The vertical formulation consists of 31 terrain-following half-sigma levels, with 11 levels in the lowest 1000 m to capture the complex interactions in the planetary boundary layer. The lowest half-sigma level is about 13 m above the surface at sea level. The model top is set at a pressure of 10 hPa with a rigid lid upper boundary. The model topography is interpolated from the 1 km resolution RADARSAT Antarctic Mapping Project Digital Elevation Model v. 2 (Liu *et al.* 2001), the so-called RAMP DEM. The regions spanned by the Ronne/Filchner ice shelf and Ross ice shelf are specified as land ice.

The Polar MM5 is initialized once-daily at 0000 UTC for each day from 1 January 1979 to 31 August 2002 (the ERA-40 dataset ends at this time). Each forecast extends out to 42 hours. Hours 24 (00Z day+1), 30 (06Z, day+1), 36 (12Z, day+1) and 42 (18Z, day+1) of each of the approximately 8600 forecasts are joined together to form a continuous 6 h dataset spanning an approximately 24 year period. The first 24 hours of the forecast are discarded to allow for spin-up of the model hydrologic cycle.

As mentioned earlier, 2 sets of approximately 24 year simulations are performed, one with initial and boundary conditions from ERA-40 (Uppala *et al.* 2005, henceforth, E40) and the other with initial and boundary conditions from NCEP-II (Kanamitsu *et al.* 2002, henceforth, NN2). A description of each of these datasets with respect to its skill over Antarctica is given below. The resolution of the data provided to Polar MM5 from both E40 and NN2 is 2.5° latitude×2.5° longitude. The variables provided for the initial and lateral boundary conditions are three-dimensional temperature, pressure, meridional and zonal winds, vertical winds and specific humidity. Sea ice fraction and land

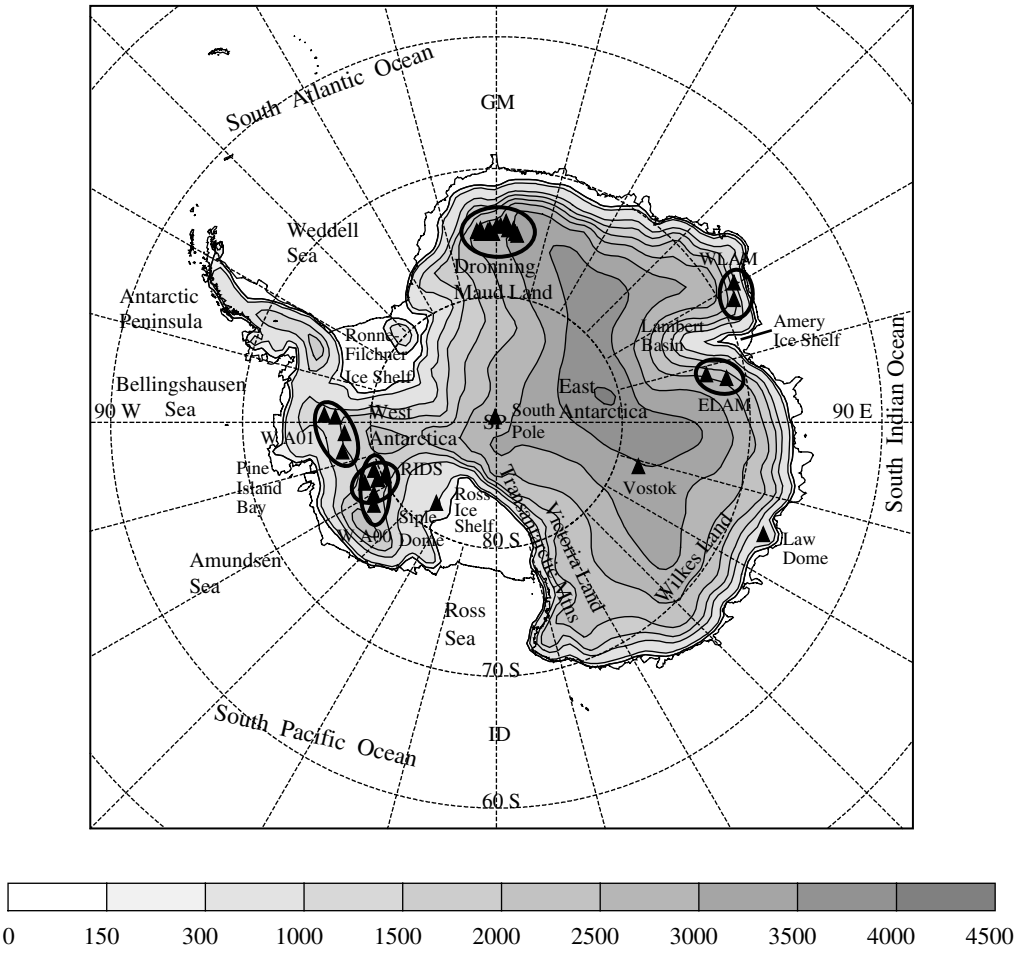

Figure 1. Polar MM5 60 km domain and topography used in this study. Topography contours are shaded. Ice core and snow stake sites are indicated by triangles (clusters of related sites are circled). Locations of common locations and features are also shown.

surface/sea surface temperatures are provided at the lower model boundary. The boundary conditions are updated at 6 hourly intervals throughout the forecast. Daily polar gridded sea ice concentration data with 25 km horizontal resolution derived from satellite passive microwave data and obtained from the US National Snow and Ice Data Centre are used to identify the sea ice surface type and its fractional coverage at each model grid point in both sets of runs. Sea surface temperatures in both sets of runs are provided by the 1.125° latitude by 1.125° longitude sea surface temperature dataset used in E40 (Fiorino 2004). This dataset uses (i) the monthly mean HadISST dataset from the United Kingdom Meteorological Office Hadley Centre for 1956–1981; and (ii) the weekly NCEP 2DVAR data for 1982—present, and is thought to be of better quality than previous datasets (Fiorino 2004).

Bromwich & Fogt (2004) evaluated mean sea-level pressure (MSLP), 2 m temperature and 500 hPa geopotential height in E40 for 1958–2001. They found

that the assimilation system is strongly constrained by satellite data, and thus performs relatively poorly over Antarctica until the modern satellite era, about 1979, and performs with good skill thereafter. Van de Berg *et al.* (in press *a*) find similar results for E40 precipitation—their results indicate a large jump in mean annual precipitation of approximately 30 mm in about 1979, with the magnitude of precipitation thereafter matching other estimates more closely.

NN2 was intended to be an improvement over the NCEP/NCAR Reanalysis (Kalnay *et al.* 1996). Over Antarctica this meant correcting a problem with the assimilation of the Australian Surface Pressure Bogus Data for the Southern Hemisphere from 1979 to 1982 (Kistler *et al.* 2001), and using improved sea ice and sea-surface temperature fields (Kanamitsu *et al.* 2002). The NCEP/NCAR Reanalysis was subject to spurious trends in MSLP and geopotential height into the 1990s in the Antarctic coastal regions due to the increase in the amount of observations assimilated into the system with time (Marshall & Harangozo 2000; Hines *et al.* 2000). Although Guo *et al.* (2004) note a 3–4 hPa drop in MSLP and a corresponding 30–40 m drop in 500 hPa geopotential height at Leningradskaya in NN2 during 1988 that may be related to a station height error, overall the spurious trends are reduced in NN2 in the period of overlap with the NCEP/NCAR Reanalysis after 1979 (Hines *et al.* 2000; fig. 5). Hines *et al.* (2000) also show the NCEP/NCAR Reanalysis captures the interannual variability of MSLP with good skill after 1979, and that the skill of NN2 is similar.

The 1985–2001 period is chosen to evaluate precipitation trends, rather than the entire 1979–2001 period, because agreement between the precipitation simulations for 1979–2001 is not as good as for other climatological variables. The two sets of simulations appear to be especially sensitive to moisture fluxes from E40 and NN2 through the lateral boundaries of Polar MM5 between about 45 and 57° S (figure 1). There are differences in the trends of the poleward moisture fluxes at these latitudes that appear to be largest before approximately 1985. The reason for this may be related to adjustments in the E40 assimilation system after the onset of the modern satellite era and prior to the mid-1980s. There is evidence of such issues in E40 prior to the mid-1980s. Turner *et al.* (in press) note that good agreement between the number of precipitation days observed at Faraday/Vernadsky station on the Antarctic Peninsula compared to the number of precipitation days from E40 does not occur until 1984 onwards. They attribute this to a lack of humidity data being assimilated into the analysis system in E40. Simmons *et al.* (2004) found that the near-surface air temperature over the Southern Hemisphere in E40 did not coincide well with that from an observationally based dataset until approximately 1987 (however, for Antarctica, agreement was good from 1979 onward). Presumably, much of the discrepancy was due to the data-sparse regions in the Southern Ocean, where the Polar MM5 boundaries are located.

In summary, the E40 and NN2 datasets appear to have adequate representations of climatological fields (near-surface temperature, MSLP and 500 hPa heights) over Antarctica during the January 1979–August 2002 period. However, the hydrologic cycle in the two datasets does not converge until the mid-1980s; thus we choose the period 1985–2001 to evaluate precipitation trends. It is noteworthy that E40 and NN2 are both based on similar observational data sources. Therefore, the main differences between the two are due to differences in

data assimilation techniques and model formulation and it must be considered when comparing the PMM5_E40 and PMM5_NN2 simulations that they are not entirely independent.

3. Comparison of simulated and observed accumulation

A comparison of the Polar MM5 E40 (PMM5_E40), Polar MM5 NN2 (PMM5_NN2), E40, NN2 and the Japanese 25 year Reanalysis (JRA) precipitation-minus-sublimation (P−E) with observed accumulation at several ice core and snow stake sites around Antarctica is shown in figure 2. The PMM5_E40 and PMM5_NN2 P−E have been interpolated from the four nearest grid points to the observation location from their nominal 60×60 km polar stereographic grids. The E40, NN2 and JRA P−E have been re-gridded to 1° latitude×1° longitude grids from their nominal output resolution, approximately 125 km for E40 and JRA and approximately 200 km for NN2, and then similarly interpolated to the location of the observation. The JRA data are included in this analysis because it has been released only recently and this is the first time its precipitation can be evaluated over Antarctica. We will use it later in the paper to provide an additional assessment of continent-wide trends in precipitation.

A considerable amount of noise can be present in ice cores due to small-scale perturbations caused by the interaction between the local topography and the wind, which can have a substantial effect on annual accumulation at a given site and mask the 'true' accumulation signal for the region as a whole (Frezzotti *et al.* 2005; Genthon *et al.* 2005). Frezzotti *et al.* (2005) note that the local spatial variability of ice core accumulation can be an order of magnitude higher than the temporal variability on decadal time-scales, which they attribute mainly to wind-driven processes. Thus, we attempt to reduce noise where possible by averaging cores together if they are in the same region, and also by averaging the first and last 5 years of the records for our comparison. The locations of the accumulation regions from figure 2 are shown in figure 1. Citations, abbreviations and temporal coverage of the observations are given in table 1. The accumulation signal at the snow stake networks at Vostok and South Pole is less noisy, as the spatial variability is already removed by averaging many stakes together. At Law Dome and Siple Dome, data are available for only one core and thus regional averaging cannot be used. However, the relatively high correlation between the simulated P−E and observed accumulation at these sites suggests that their locations at the tops of ice domes may reduce the amount of small-scale perturbation in the cores, and thus we include them in the analysis. Overall, the correlation coefficients between the simulated and observed records (figure 2*c*) indicate that the modelled and observed annual accumulation variability share common variance different from zero at the 90% confidence interval at many of the sites (especially in West Antarctica), despite the small-scale perturbations in the observational records. Though these relationships are often weak, they are as good as can be expected considering the differences between the simulated and observed accumulation signals, and thus we consider the following comparison to be valid. The 90% confidence interval is used to test statistical significance throughout the remainder of this paper. This value has been chosen, rather than

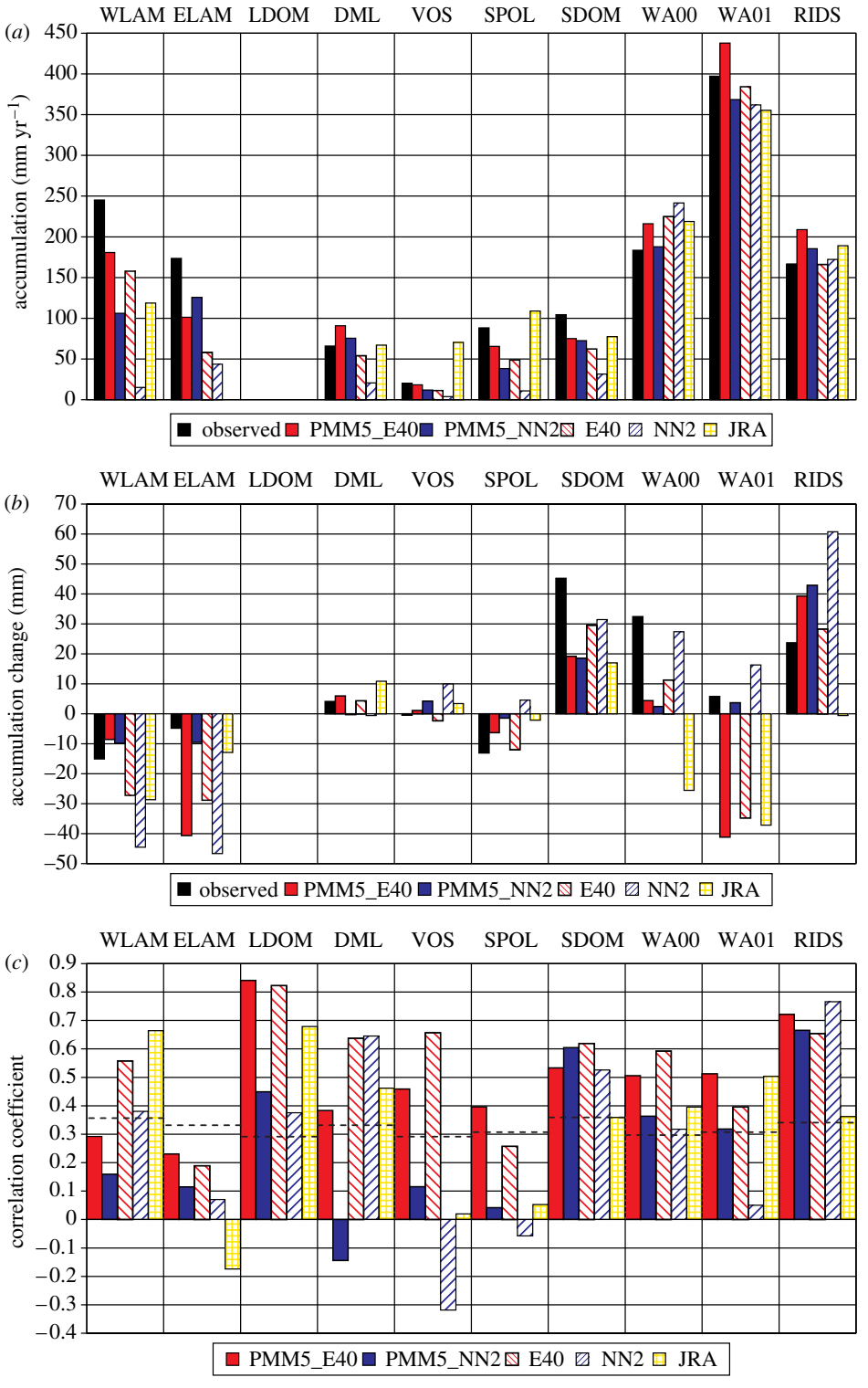

Figure 2. (*Caption opposite.*)

Figure 2. (*Opposite.*) Comparison of annual accumulation records from ice cores and stake networks to simulated P−E from PMM5_E40, PMM5_NN2, E40, NN2 and JRA. The simulated P−E is interpolated to the location of the observation. Where possible, ice core records have been averaged together by region to reduce noise. The regions are defined in table 1 and shown in figure 1. (*a*) Mean accumulation for the 10 years encompassing the first 5 years (1985–1989) and the last 5 years of the record (period varies depending on the length of the observational record—see table 1). (*b*) Change (mm) between first and last 5 years of each record. (*c*) Correlation coefficient of observed versus simulated annual accumulation from 1985 to the end of the record (dashed lines indicate the correlation is significantly different from zero at the 90% CI). The mean accumulation and changes at Law Dome are not shown because they are not published as of this writing (Tas van Ommen 2005, personal communication).

Table 1. Ice core and snow stake records used in this study and shown in figure 2.

source of accumulation observation	abbreviated name in figure 2	approximate location (see figure 1)	length of record
average of western Lambert Basin cores LGB00 and MGA (Goodwin *et al.* 1994; Higham & Craven 1997; I. D. Goodwin 1995 unpublished thesis)	WLAM	68.6° S, 61° E	1985–1994
average of eastern Lambert Basin cores DT085 (Xiao *et al.* 2001) and DT001 (Wen *et al.* 2001)	ELAM	72° S, 77.5° E	1985–1996
Law Dome core DSS97 used for 1985–1996 and core DSS0405 used for 1997–2001 (Tas van Ommen unpublished)	LDOM	66.8° S, 112.8° E	1985–2001
average of 13 firn cores from Dronning Maud Land (Oerter *et al.* 2000)	DML	75° S, 0° E	1985–1996
Vostok stake network (Ekaykin *et al.* 2004)	VOS	78.5° S, 106.9° E	1985–2001
South Pole core used for 1985–1989 (Meyerson *et al.* 2003) and stake network for 1995–1999 (Mosley-Thompson *et al.* 1999)	SPOL	90.0° S, 0.0° E	1985–1999
Siple Dome core (Nereson *et al.* 1996)	SDOM	81.7° S, 149.0° E	1985–1994
average from West Antarctic firn cores 00–1, 00–4 and 00–5 (Kaspari *et al.* 2004)	WA00	79° S, 115° W	1985–2000
average from West Antarctic firn cores 01–2, 01–3, 01–5 and 01–6 (Kaspari *et al.* 2004)	WA01	78° S, 95° W	1985–1999
average from West Antarctic firn cores RIDS-A, RIDS-B, and RIDS-C (Kaspari *et al.* 2004)	RIDS	79° S, 118° W	1985–1995

the 95 or 99% interval, to permit substantial changes to be more easily recognized over the relatively short time intervals evaluated.

The mean annual P−E in the western and eastern Lambert basin in all simulations is lower than observed. The NN2 accumulation is particularly low; this is due to unrealistically large sublimation (Hines *et al.* 1999) in the model that occurs over most of the coastal and interior locations in East Antarctica, but is not an issue in West Antarctica. Unrealistically large sublimation is also present in the JRA record in ELAM, causing accumulation of approximately 0 mm yr^{-1} and a negative correlation coefficient. PMM5_E40 and E40 provide the most realistic estimates of mean accumulation in both basins and have the highest correlation

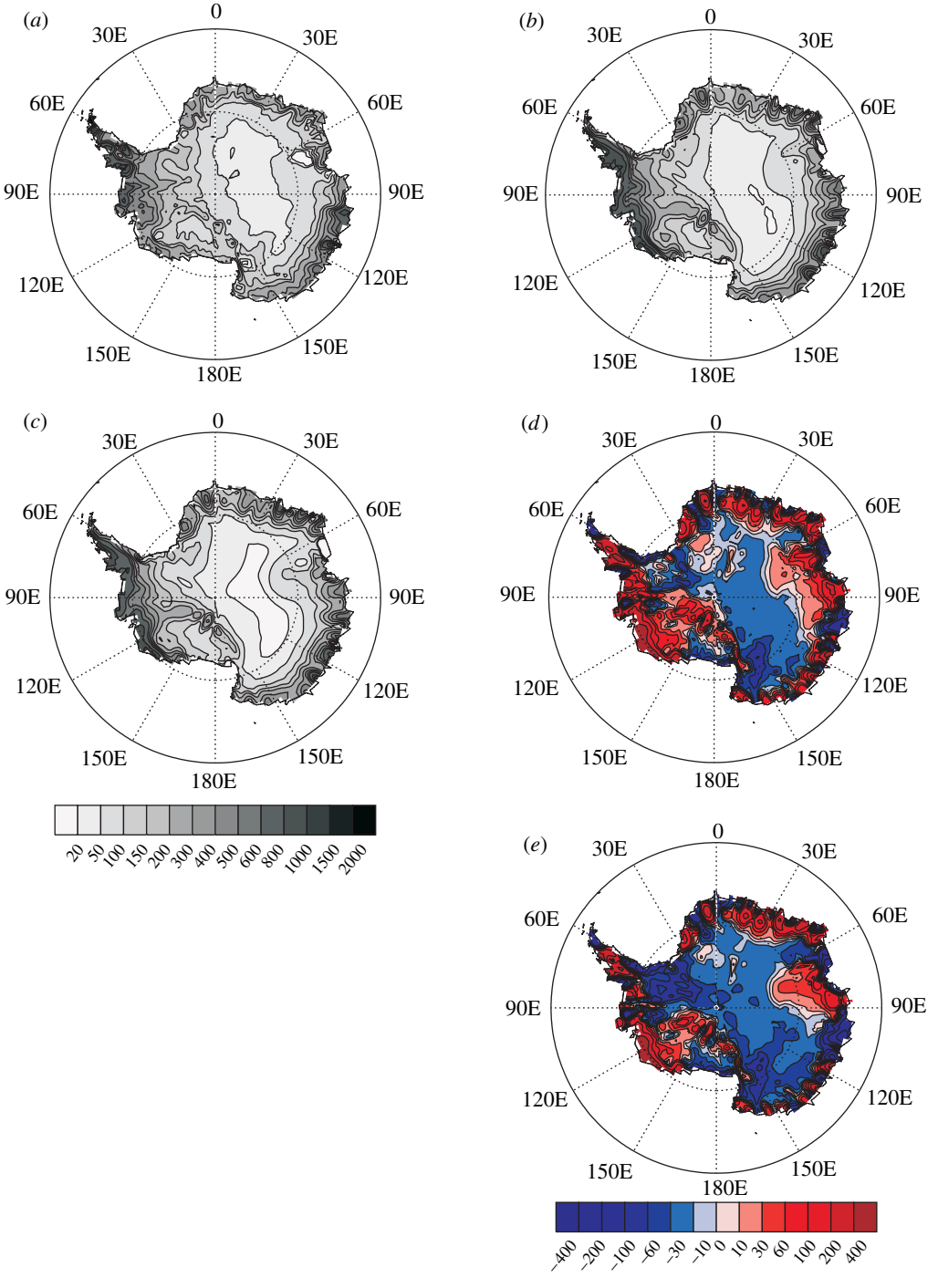

Figure 3. Long-term accumulation distribution (mm yr^{-1} water equivalent) from (*a*) Vaughan *et al.* (1999), (*b*) 1985–2001 PMM5_E40 P-E, (*c*) 1985–2001 PMM5_NN2 P-E, (*d*) Vaughan minus PMM5 E40 and (*e*) Vaughan minus PMM5 NN2.

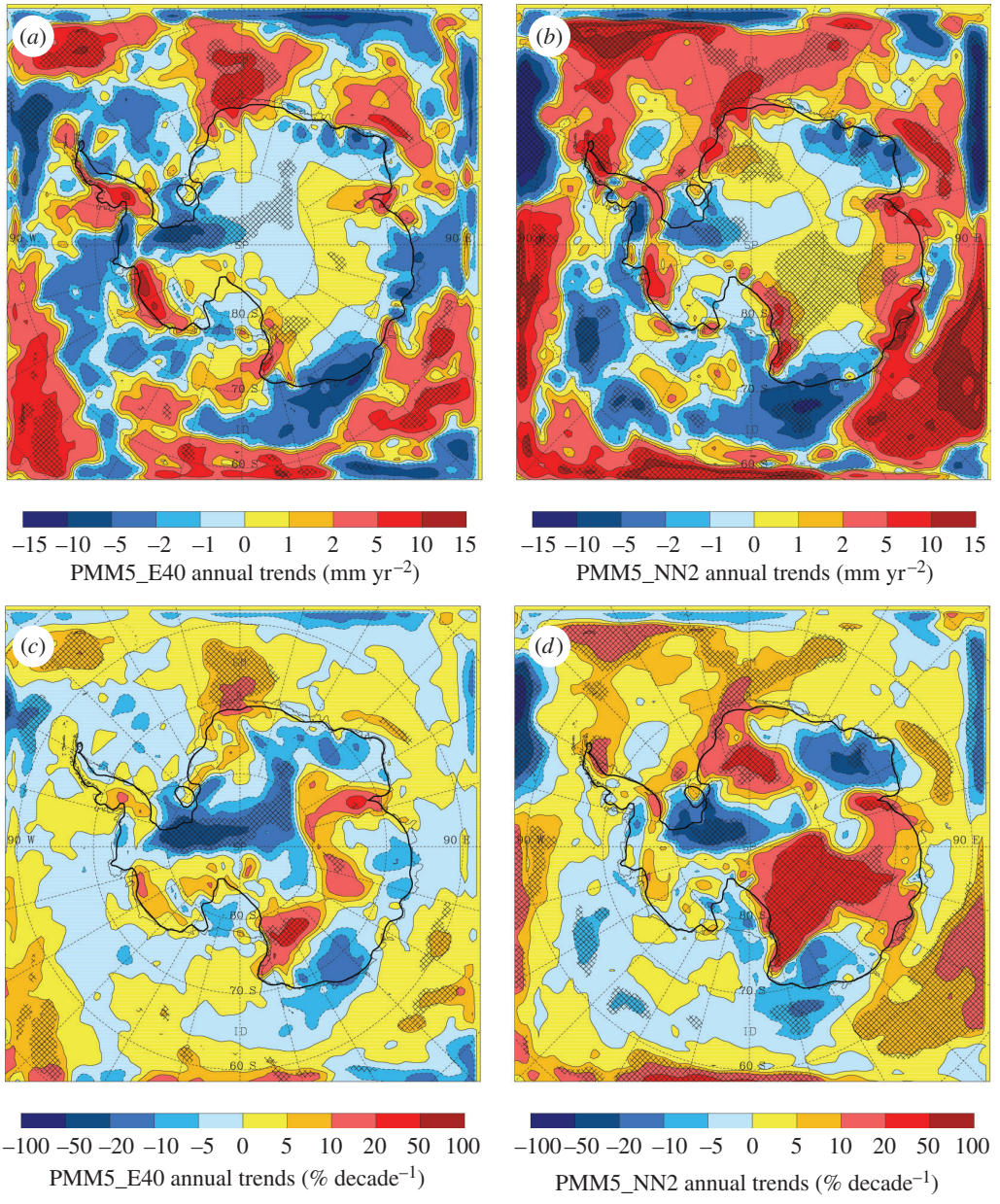

Figure 4. Annual precipitation trends (mm yr^{-2}) for 1985–2001 derived from a linear fit through each grid point for the (*a*) PMM5_E40 and (*b*) PMM5_NN2 runs. (*c*) and (*d*) are the same as (*a*) and (*b*), but expressed as percent change per decade. Hatching indicates the trend is significantly different from zero at the 90% confidence interval.

coefficients (with the exception of JRA in WLAM). All of the models capture the observed negative change in accumulation at these two sites. At Law Dome, the P−E in all of the models correlates well with the observed accumulation. Mean annual accumulation and temporal changes cannot be shown for Law Dome as the data have yet to be published (Tas van Ommen 2005, personal

communication). However, it is noteworthy that only PMM5_E40 and E40 capture the correct sign of the changes there. In Dronning Maud Land all of the models, with the exception of NN2, simulate the mean P−E well. PMM5_E40, E40 and JRA capture the temporal change, but PMM5_NN2 and NN2 do not. PMM5_E40 simulates the mean P−E at Vostok most closely, and is also closest to the near zero temporal change observed there. PMM5_NN2, NN2 and JRA predict relatively large positive changes (as a percentage of mean accumulation) that do not appear in the Vostok record. The correlation coefficients indicate that PMM5_E40 and E40 capture interannual variability at Vostok with the most skill; the negative correlation coefficient in the NN2 P−E is due to the overestimation of the sublimation fluxes. At South Pole, the models underestimate P−E, with the exception of JRA, which overestimates accumulation over the entire interior of the ice sheet. All of the models except NN2 capture the negative temporal change at South Pole. The correlation coefficients indicate that PMM5_E40 demonstrates some skill in simulating interannual variability at South Pole, while the other datasets show almost no skill.

At the four remaining sites, all in West Antarctica, the simulated P−E is similar to the observed accumulation for all of the models. The temporal changes at all four sites are captured in PMM5_NN2 and NN2, and at three out of four sites in PMM5_E40 and E40. The JRA model captures the temporal change at one of the four sites. Near Pine Island Bay (WA01) where large changes in accumulation (Kaspari *et al.* 2004) and ice volume (Rignot & Thomas 2002; Thomas *et al.* 2004) have been measured recently, PMM5_E40, E40 and JRA fail to capture temporal change despite resolving the mean accumulation and interannual variability reasonably well.

Overall, the PMM5_E40 and E40 simulated P−E capture the mean accumulation, temporal changes and interannual variability over the continent as a whole with the most skill. PMM5_E40 predicts higher P−E than E40 at nearly every site, and in most cases this is closer to the observed accumulation. Both predict the temporal changes in nearly every instance, with the exception of the WA01 region. In general, it cannot be said that the hydrologic cycle in PMM5_E40, with its higher resolution and polar physics, substantially improves on E40, the model that provides its initial and boundary conditions. The PMM5_NN2 and NN2 tend to underestimate P−E over East Antarctica, and do not capture interannual variability as well as PMM5_E40 and E40. Over West Antarctica, the skill of PMM5_NN2 and NN2 is comparable to PMM5_E40 and E40. Unlike PMM5_E40 versus E40, the hydrologic cycle in PMM5_NN2 improves estimates of P−E compared to NN2, being closer to the observed accumulation at all sites with the exception of RIDS. PMM5_NN2 also captures the magnitude of temporal changes better than NN2, and captures interannual variability better than NN2 at seven out of ten sites. The JRA model shows promising skill in capturing variability and trends at some locations (WLAM and DML), but is inconsistent overall, incorrectly depicting the sign of the temporal changes in five of the ten regions. For the remainder of this section, and in §4, we will assess the spatial variability and trends of accumulation using PMM5_E40 and PMM5_NN2. Based on the findings above, the use of these two simulations is a reasonable choice: PMM5_E40 and E40 capture the mean, temporal change and interannual variability of Antarctic accumulation with similar skill, and thus it is only necessary to show one of the two; of the remaining runs, PMM5_NN2

shows the best overall skill at depicting variability and trends versus NN2 and JRA, yet it is different enough from PMM5_E40 to provide a useful comparison.

Figure 3 compares the Vaughan *et al.* (1999) accumulation compilation, which is a synthesis of accumulation observations taken over many years, with the P − E from the PMM5_E40 and PMM5_NN2 runs. The broad features of Antarctic accumulation are captured in both of the Polar MM5 runs, with maxima in the coastal areas, especially West Antarctica and the Antarctic Peninsula, and a large area within the continental interior with accumulation of less than 50 mm yr^{-1}. The interior accumulation in the PMM5_NN2 runs appears to be less than the Vaughan *et al.* (1999) or the PMM5_E40 datasets. This is confirmed by comparing figure 3*d* and *e*. Here it is seen that PMM5_NN2 is dryer than PMM5_E40 in the continental interior. Figure 3*d* and *e* also reveal a general characteristic of both datasets: they are dryer than the Vaughan *et al.* (1999) dataset in the interior and wetter in the coastal regions. Bromwich *et al.* (2004) discuss the dry bias in the interior and relate this to the limited ability of Polar MM5 to represent clear sky precipitation, which Bromwich (1988) infers to form nearly continuously in the interior of Antarctica without organized synoptic processes. In Victoria Land, the dry bias in PMM5_E40 and PMM5_NN2 may be exaggerated, as ice core and snow stake evidence from recent studies indicates that the Vaughan *et al.* (1999) dataset overestimates accumulation in this region on average by 33%, and by as much as 65% in some areas (Frezzotti *et al.* 2004; Magand *et al.* 2004). In the coastal regions, a recent study by Van de Berg *et al.* (in press *b*) compares the Vaughan *et al.* (1999) dataset to several hundred observations and concludes that the compilation generally underestimates coastal precipitation. Our comparison with coastal ice core records in the previous paragraph also corroborates this conclusion, as we generally find that our simulated accumulation is of the order of, or less than, the long-term ice core accumulation. In summary, the spatial distribution of the PMM5_E40 and PMM5_NN2 P − E matches that in the long-term accumulation compilation of Vaughan *et al.* (1999), and the magnitude of long-term annual mean P − E is accurate within the bounds of uncertainty.

In summary, the PMM5_E40 and PMM5_NN2 simulations largely depict the observed spatial and temporal variability of Antarctic precipitation, especially considering the small-scale perturbations that are not resolved in the models but likely exist in the observational records despite space/time filtering where possible. The PMM5_E40 record appears to be most reliable for resolving the mean accumulation, variability and trends, particularly in East Antarctica. In the following section, the spatial distribution of the temporal trends of precipitation is examined using these two datasets. From henceforth, precipitation, rather than P − E, is used. Precipitation is the dominant term in Antarctic accumulation (Bromwich 1988) and it has been shown that over broad space scales as considered here, precipitation can be largely transposed to the surface mass balance (Genthon 2004).

4. Spatial distribution of the temporal trends of precipitation for 1985–2001

Figure 4 shows the spatial distribution of the 1985–2001 linear trends for the PMM5_E40 and PMM5_NN2 annual precipitation. Figure 4*a* and *b* express the

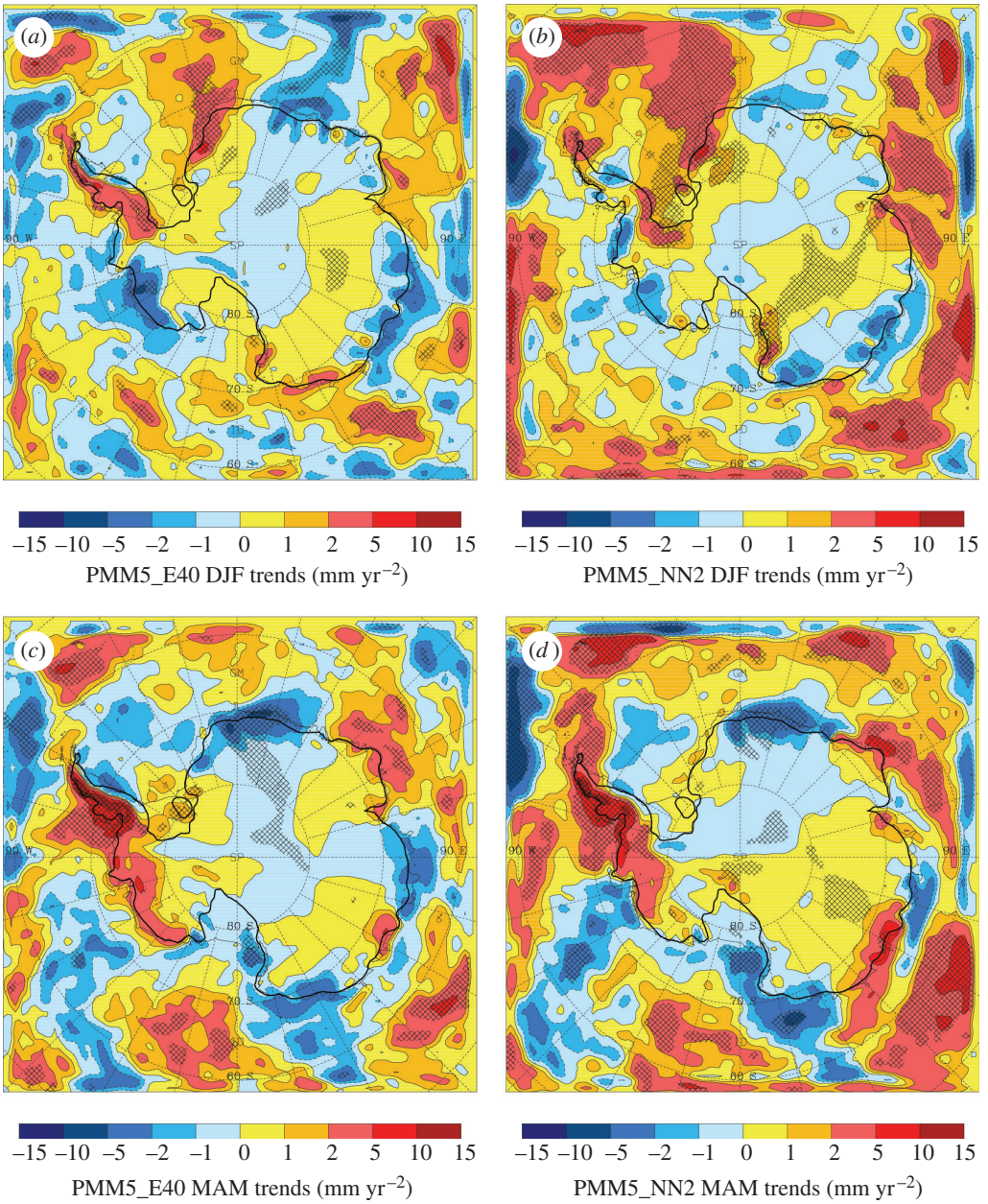

Figure 5. Seasonal precipitation trends (mm yr^{-2}) for 1985–2001 derived from a linear fit through each grid point for the (*a*) PMM5_E40 DJF, (*b*) PMM5_NN2 DJF, (*c*) PMM5_E40 MAM and (*d*) PMM5_NN2 MAM runs. Hatching indicates the trend is significantly different from zero at the 90% confidence interval. The DJF trends begin in December 1985 and end in February 2002.

trends in mm yr^{-2}, and figure 4*c* and *d* express the same trends in percent per decade, which allows for the relative change to be assessed over high elevations where little precipitation falls. Areas of strong upward and downward trends are apparent. Statistically significant (at the 90% CI) upward trends are

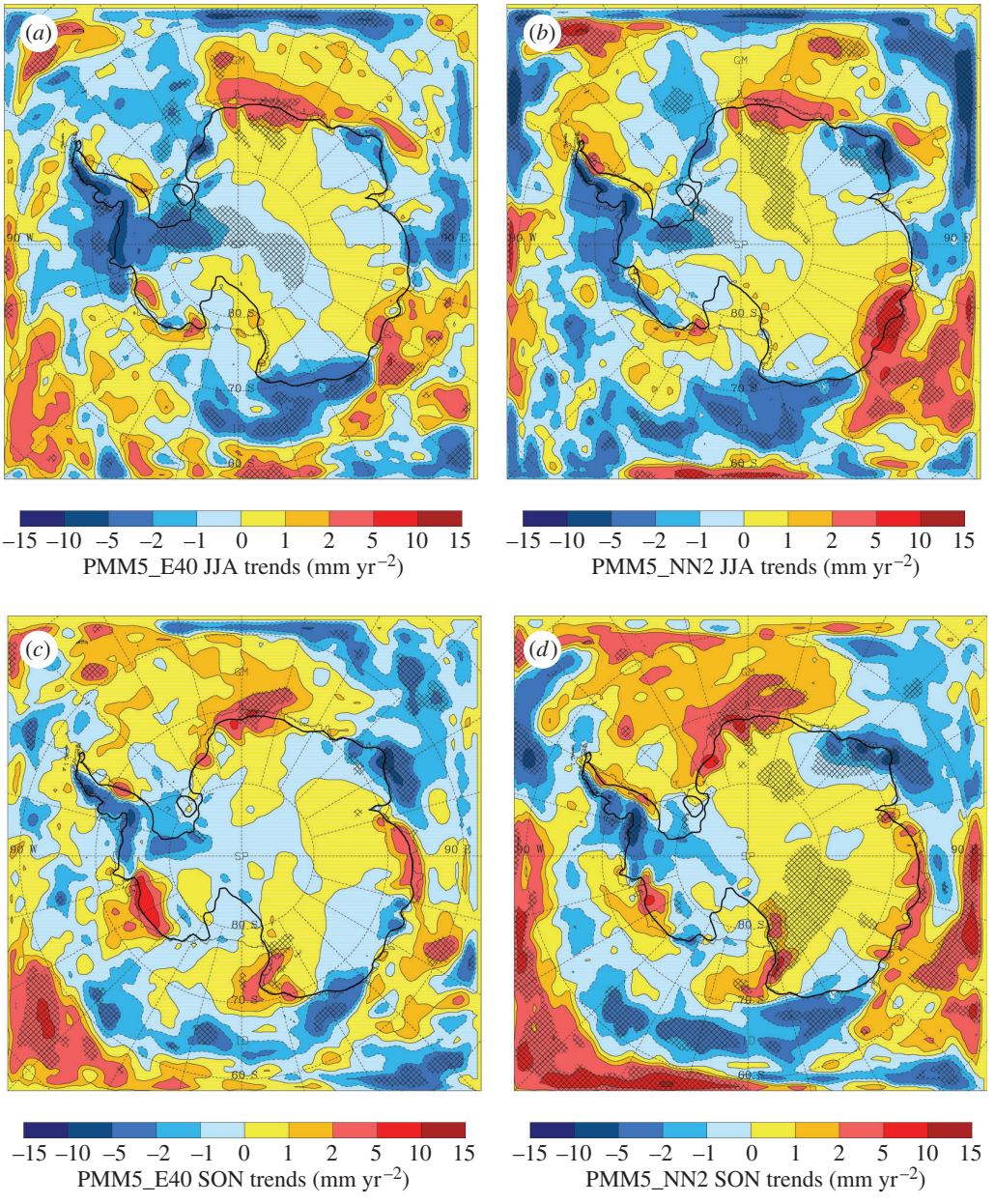

Figure 6. Seasonal precipitation trends (mm yr^{-2}) for 1985–2001 derived from a linear fit through each grid point for the (*a*) PMM5_E40 JJA, (*b*) PMM5_NN2 JJA, (*c*) PMM5_E40 SON and (*d*) PMM5_NN2 SON runs. Hatching indicates the trend is significantly different from zero at the 90% confidence interval.

occurring near the Antarctic Peninsula, in the ocean regions north of the coastline at approximately 0° E and between 105° and 150° E, and in the Transantarctic Mountains in Victoria Land. Statistically significant downward trends are occurring just inland of the Ronne-Filchner ice shelf. Strong

downward trends are also indicated in coastal regions of East Antarctica in both simulations, although these are, for the most part, not statistically significant. Overall, there is broad agreement between the two simulations, but the regions of positive change in the PMM5_NN2 simulations are larger. A broad region of 20–50% change-per-decade over East Antarctica is indicated in the PMM5_NN2 runs (figure 4*d*), but considering that this model tended to overestimate positive precipitation changes at Vostok (figure 2), the smaller PMM5_E40 trends (figure 4*c*) are likely to be more representative of precipitation changes over East Antarctica.

Figures 5 and 6 are similar to figure 4*a* and *b*, but for the four seasons: summer (DJF, figure 5*a*,*b*), autumn (MAM, figure 5*c*,*d*), winter (JJA, figure 6*a*,*b*), and spring (SON, figure 6*c*,*d*). In DJF, both datasets show positive precipitation trends over the Antarctic Peninsula, the Ronne-Filchner ice shelf, and much of the sector between 0° E and 90° W. Both datasets also indicate strong and often significant trends over the region of East Antarctica near Vostok, and in ocean areas adjacent to coastal East Antarctica. In MAM, the spatial patterns of the trends are similar to those in DJF, except in the Weddell Sea where there is a larger area of negative trends, and over coastal West Antarctica where the trends become positive. The positive trends in MAM over the Antarctic Peninsula are stronger than in DJF. In JJA, the precipitation trends are strongly negative in the Bellingshausen Sea and over the Antarctic Peninsula, although there is a region of positive trends on the east side of the Peninsula. Broad, statistically significant negative trends are also present near the coast at 45° E, and in the ocean regions of the South Pacific between 135° W and 135° E. An area of strong positive change is located along and inland of the coast near 0° E. The spatial distribution of the trends in SON is similar to JJA, except in the Weddell Sea, where the trends become positive in SON. Over the continent as a whole, the trends are more positive in SON than in JJA. Regions of consistent positive change in all four seasons are apparent over much of the interior of East Antarctica between 90 and 180° E, and in the ocean areas north of 0 and 120° E. There are few areas where negative trends are present in all four seasons.

Figure 7 summarizes the annual and seasonal trends shown in figures 4–6 by averaging them into broad regions. All of the averages are taken over land/ice shelf grid points only, except for the 'ALL' category, which includes the entire domain (ocean + land grid points). We show the precipitation trends over the GIS in figure 7, but reserve a detailed discussion of this important region for §5. The trends over the Ronne-Filchner ice shelf and the Antarctic Peninsula are positive in summer and autumn, and negative in winter and spring. There are no significant trends over the Ross Ice Shelf or West Antarctica annually or in any season, and a significant positive trend is present in East Antarctica only in spring in the PMM5_NN2 precipitation. Significant positive trends are present over the entire domain in summer and autumn. It is interesting that the trends over the Peninsula, the Ronne-Fichner Ice Shelf, and the entire domain closely follow trends in the Southern Annular Mode (SAM, Marshall 2003). The SAM can be thought of as the measure of the strength of the pressure gradient between the mid-latitudes and high latitudes, from about 40 to 65° S (e.g. Thompson & Wallace 2000; Marshall 2003; Fogt & Bromwich 2006). The upward precipitation trends in the summer and autumn coincide with a strengthening of the SAM in these seasons, and the downward trends in winter coincide with a weakening of

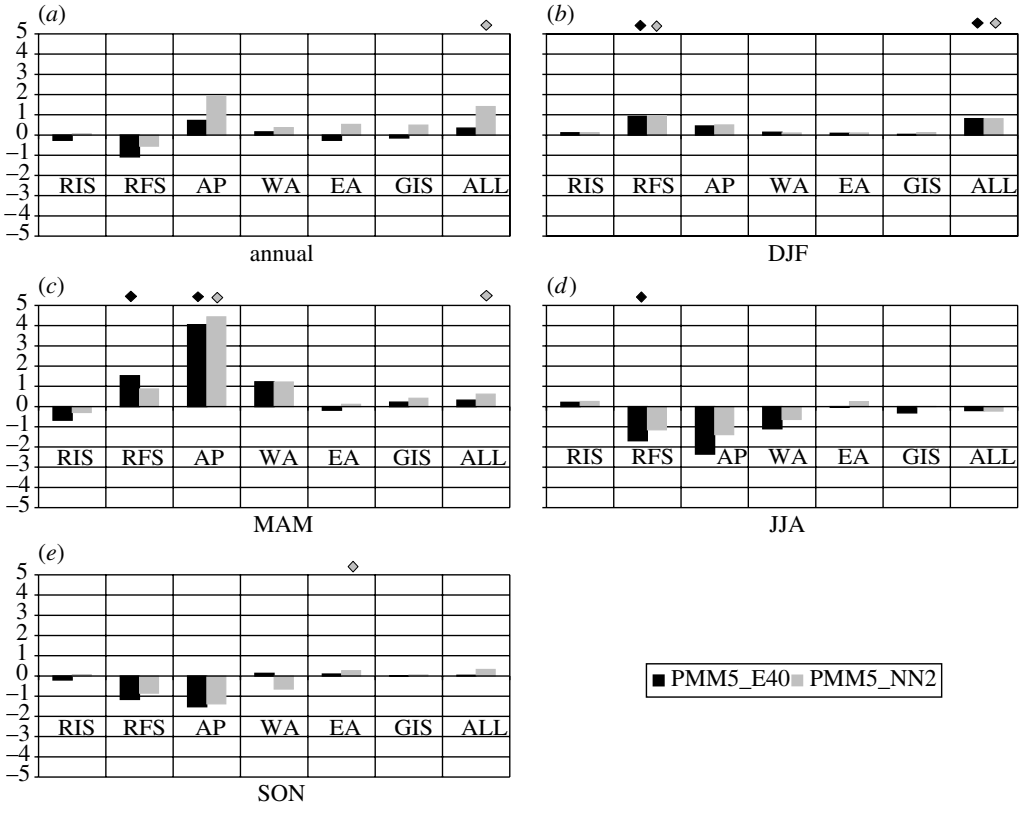

Figure 7. Regionally averaged annual and seasonal precipitation trends (mm yr^{-2}) for 1985–2001. The regions are RIS, Ross Ice Shelf; RFS, Ronne-Filchner Ice Shelf; AP, Antarctic Peninsula; WA, West Antarctica; EA, East Antarctica; GIS, grounded ice sheet and ALL, entire model domain. Only land/ice shelf grid points are included in the averages, except for 'ALL'. A diamond above a bar indicates the trend is significantly different from zero at the 90% confidence interval.

the SAM in this season (although this weakening is not present in all proxies of the SAM). Turner *et al.* (in press) also infer a strong increase in precipitation over the Antarctic Peninsula since 1950 from the record of observed precipitation days at Faraday/Vernadsky (65.25° S, 64.27° W), especially in summer and autumn, and link this to the strengthening of the SAM during DJF and MAM. Although there are smaller downward trends over the Peninsula and Ronne-Filchner ice shelf in spring, there is little trend in the SAM during this season, as it is thought that the SAM is damped by the El Niño-Southern Oscillation (ENSO) in spring (Fogt & Bromwich 2006).

In summary, the spatial distribution of the annual and seasonal precipitation trends in PMM5_E40 and PMM5_NN2 are similar despite the differences in mean accumulation and local trends discussed in §3. The annual trends tend to be a small residual of seasonal trends that exhibit a large degree of interseasonal variability. Marshall *et al.* (2004) demonstrated that the trends in the SAM for the annual mean and austral summer are unlikely to be due to internal climate variability alone, and that anthropogenic forcing also plays a role. Considering

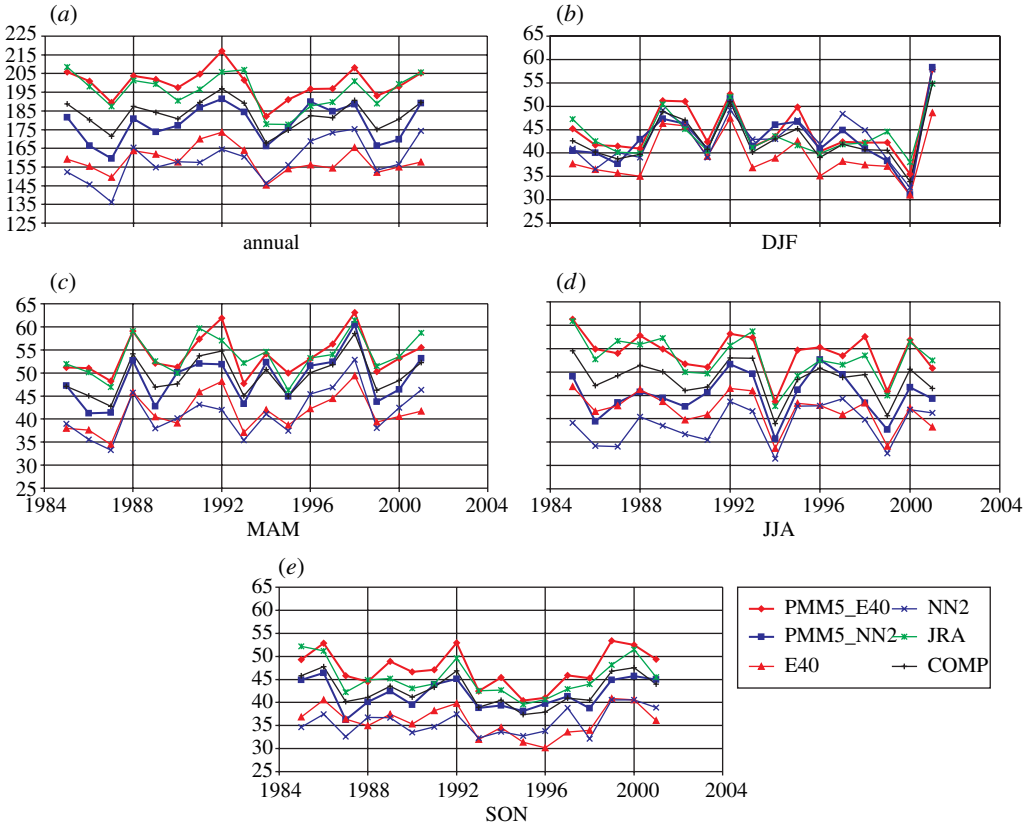

Figure 8. Time-series of annual and seasonal forecast precipitation over the GIS (mm yr^{-1}) for the two sets of Polar MM5 runs as well as E40, NN2, JRA and the composite ('COMP') of PMM5_E40, PMM5_NN2, E40 and JRA.

the relationship between seasonal precipitation trends and the SAM noted here, this suggests that some of the regional precipitation trends may be related to human-induced climate changes.

5. Precipitation trends over all of Antarctica for 1985–2001

Figure 8 shows the 1985–2001 annual and seasonal Antarctic-wide precipitation (mm yr^{-1}) averaged over the GIS for PMM5_E40, PMM5_NN2, E40, NN2, JRA and the composite ('COMP') of PMM5_E40, PMM5_NN2, E40 and JRA. NN2 is not included in the composite because of its relatively poor ability to capture temporal changes over much of the interior of the ice sheet (figure 2, DML, VOS, SPOL), and its tendency to substantially overestimate changes at WLAM, ELAM, WA01 and RIDS. To make the comparison uniform, all of the datasets have been interpolated to a 1° latitude×1° longitude grid. Grounded ice sheet grid points are defined as falling within the land mask of Vaughan *et al.* (1999) and being above the 300 m elevation contour of the Polar MM5 topography interpolated to the same grid, which largely eliminates ice shelf grid points

Table 2. Summary table of precipitation means and trends for the grounded ice sheet (GIS) corresponding to the time-series in figure 8. 'COMP' is the composite of the PMM5_E40, PMM5_NN2, E40 and JRA time-series. Bold trends are significantly different from zero at the 90% confidence interval.

category	season	PMM5_E40	PMM5_NN2	E40	NN2	JRA	COMP
1985–2001 mean ($mm\ yr^{-1}$)	ANNUAL	200	178	158	159	195	183
	DJF	45	43	39	43	44	43
	MAM	54	49	41	41	54	49
	JJA	54	45	42	39	53	49
	SON	47	42	36	36	45	43
1985–2001 trend ($mm\ yr^{-2}$)	ANNUAL	−0.16	0.49	−0.21	**1.20**	−0.29	−0.04
	DJF	0.02	0.13	0.01	0.30	0.03	0.05
	MAM	0.20	0.40	0.25	**0.51**	0.25	0.28
	JJA	−0.30	0.00	**−0.34**	0.25	**−0.37**	−0.25
	SON	−0.01	0.05	−0.08	0.20	−0.13	−0.04
% difference of mean precipitation for 1997–2001 from 1985 to 1989	ANNUAL	0	4	−1	10	−1	1
	DJF	0	2	1	8	1	1
	MAM	6	13	9	17	7	9
	JJA	−7	0	−11	7	−9	−7
	SON	2	3	−1	7	−2	1

(the 300 m contour of the Polar MM5 topography, which is based on the RAMP DEM, is shown in figure 1). Using this technique, the surface area of the GIS is 11 960 000 km^2, nearly identical to the 11 966 000 km^2 area calculated by Vaughan *et al.* (1999). This technique also includes the northern area of the Antarctic Peninsula that is not part of the GIS, as precipitation falling on this region will affect the global sea level budget.

Both the PMM5_E40 and PMM5_NN2 runs predict higher precipitation than the respective reanalyses used to drive them, E40 and NN2; this is at least partly due to higher horizontal resolution in Polar MM5, especially along the steep coastal margins where the majority of precipitation falls. Overall, the annual and seasonal precipitation variability among the datasets is in relatively good agreement. The amount of JRA precipitation is very similar to that in PMM5_E40, although this relationship appears to be a result of spatial averaging. JRA overestimates precipitation on the high plateau and underestimates it in coastal regions when compared to PMM5_E40.

Table 2 summarizes the annual and seasonal precipitation means and trends for the GIS for the time-series shown in figure 8. The percent difference between the first 5 years and last 5 years of the record is also presented as an alternate means of assessing precipitation change for this relatively short time-period. The precipitation change expressed in this manner is in good agreement with the 1985–2001 linear trends. The mean annual precipitation ranges between 158 (E40) and 200 $mm\ yr^{-1}$ (PMM5_E40). A recent study by Van de Berg *et al.* (in press *b*) suggests that the best estimate of accumulation over the GIS is about 171 $mm\ yr^{-1}$, substantially more than the estimate of 149 $mm\ yr^{-1}$ by Vaughan *et al.* (1999). Considering sublimation is roughly 10% of precipitation (Bromwich *et al.* 2004), the P−E in Polar MM5 would be close to this accumulation

estimate, while that in E40 would underestimate it. The maximum seasonal precipitation occurs in autumn and winter in all of the runs except NN2. Bromwich (1988) noted that the maximum precipitation over the continent falls in the winter months, and thus it is likely that the seasonal cycle of precipitation in NN2 is inaccurate.

The PMM5_NN2 trends are more positive than the PMM5_E40 trends in all cases. Likewise, the NN2 trends are always more positive than the E40 trends. The largest positive trends are found in NN2 in all seasons except autumn, in which PMM5_NN2 has the largest trend. The PMM5_E40 trends are more positive than the E40 trends in all cases except MAM, and the PMM5_NN2 trends are smaller than the NN2 trends in all cases. This makes the annual precipitation trends closer to zero in the PMM5_E40 and PMM5_NN2 datasets with respect to the E40 and NN2 datasets, even though the mean annual precipitation in PMM5_E40 and PMM5_NN2 is much larger than that in the respective 'parent' dataset of each, E40 and NN2. The JRA trends are similar to those in PMM5_E40 and E40, suggesting that the interannual variability and trends in the poleward moisture fluxes in JRA are similar to those in E40.

Collectively considered, all of the datasets predict positive trends in DJF and MAM, but there is less agreement for JJA and SON. Few trends are significantly different from zero at the 90% confidence interval. Only NN2 shows a significant positive trend for the annual precipitation, but considering the issues with this dataset noted earlier, this trend is questionable. The composite trend suggests that the annual precipitation trend over the GIS is nearly zero.

Table 3 summarizes the annual precipitation and accumulation trends discussed here, as well as results from different studies for various time-periods, and gives their contribution to global sea level. The estimates from the datasets in this study are presented in terms of P−E so that they most closely reflect their sea-level contribution (surface meltwater runoff is neglected as most meltwater refreezes near where it is produced and has been shown to have little effect on surface mass balance (Liston & Winther 2005)). The number from Bromwich & Robasky (1993) is shown, although it covers a much earlier time-period (through 1975), as a means of perspective. Their analysis was based on a sparse network of accumulation observations with numerous gaps, and may substantially overestimate the precipitation increase from 1955 to 1975. However, a large change in sea ice extent was noted between these two periods (De la Mare 1997), and thus such a large, continent-wide change may have been possible.

Contemporary estimates for the period after 1979 range from +1.67 (NN2, 1979–1999) to −0.50 mm yr^{-2} (E40, 1980–2001). Seven of the estimates predict positive trends in precipitation/accumulation, while five predict negative trends. Of the seven that predict positive trends, two of the estimates from Bromwich *et al.* (2004) are questionable, as they are based on the E15_ECT dataset, which appears to have an artificial jump in precipitation (and other fields) after 1994 that causes spurious trends. Four of the five datasets that produce negative trends are either E40 or based on E40, which have been shown above to capture variability and trends over the continent with better skill than PMM5_NN2 and NN2 when compared to ice core and snow stake records. It is noteworthy that there is a considerable difference between the mean P−E from E40 calculated by Van de Berg *et al.* (in press *a*) for the 1980–2001 period (119 mm yr^{-1}) and that calculated in this study (135 mm yr^{-1}). This appears to be largely due to our

Table 3. Summary of accumulation and precipitation trends from various studies, including this one. Uncertainties about the trends in this study are based on the 90% confidence interval. Bromwich *et al.* (2004) uncertainties were based on the 95% confidence interval, and those from Van de Berg *et al.* (in press *a*,*b*) were computed as one standard deviation about the trend. The contribution to global sea level is calculated by multiplying the trend by the ratio of the GIS surface area (1.19×10^7 km^2) to that of the global ocean (36.13×10^7 km^2). The calculation for percentage of current GSL rise is based on a GSL increase of 2.8 mm yr^{-1} (Leuliette *et al.* 2004). Note that the contribution to global sea-level rise becomes increasingly important each year, as the trend indicated is the *additional* amount of water each year compared to the previous year.

study	method		mean$\pm$s.d.	trend	uncertainty	contribution to GSL rise	% of current GSL rise
Bromwich & Robasky (1993)	moisture budget study analysing difference of accumulation between 1955–1965 and 1965–1975	P$-$E	n.a.	n.a.	n.a.	-0.200	-7.1
Bromwich *et al.* (2004)	dynamic retrieval from ERA15 reanalyses and ECMWF/TOGA operational analyses, 1979–1999	P	188 ± 10	1.65	0.8	-0.054	-1.9
Bromwich *et al.* (2004)	modelled from ERA15 reanalysis and ECMWF/TOGA operational analyses, 1979–1999	P	180 ± 15	1.35	1.1	-0.044	-1.6
Bromwich *et al.* (2004)	modelled from NN2, 1979–1999	P	180 ± 12	1.67	0.59	-0.055	-2.0
Van de Berg *et al.* (in press *a*,*b*)	modelled from E40, 1980–2001[a]	P$-$E[a]	119	-0.50	0.22	0.016	0.6
Van de Berg *et al.* (in press *a*,*b*)	modelled from RACMO2/ANT regional model, driven by E40 1980–2002[a]	P$-$E$-$M[a]	166	0.15	0.28	-0.005	-0.2
this study	modelled from Polar MM5, driven by E40, 1985–2001	P$-$E[a]	180 ± 8	-0.13	0.70	0.004	0.2
this study	modelled from Polar MM5, driven by NN2, 1985–2001	P$-$E[a]	157 ± 9	0.47	0.81	-0.015	-0.6
this study	modelled from E40, 1985–2001	P$-$E[a]	135 ± 7	-0.29	0.62	0.010	0.3
this study	modelled from NN2, 1985–2001	P$-$E[a]	84 ± 9	0.58	0.74	-0.019	-0.7
this study	modelled from JRA, 1985–2001	P$-$E[a]	155 ± 10	-0.47	0.88	0.015	0.6
this study	composite of PMM5_E40, PMM5_NN2, E40, and JRA, 1985–2001	P$-$E[a]	157 ± 8	-0.10	0.67	0.003	0.1

[a]Grounded ice sheet only.

inclusion of the northern tip of the Antarctic Peninsula in this study. There is also a discrepancy between the long-term annual NN2 precipitation from Bromwich *et al.* (2004) versus the NN2 P−E from this study (188 versus 84 mm yr^{-1}). Although these averages are calculated for slightly different surface areas, the difference is primarily due to the inclusion of sublimation in our approximation and infers that sublimation is about 100 mm yr^{-1} over the GIS, about an order of magnitude too large; this problem has been noted in previous literature for the similar NCEP/NCAR Reanalysis (Hines *et al.* 1999). For the three high spatial resolution mesoscale atmospheric models used (PMM5_E40, PMM5_NN2 and RACMO2/ANT), recent accumulation trends are not statistically different from zero.

Overall, the results from this study suggest that, when averaged over the grounded Antarctic ice sheet, recent accumulation trends may not be significantly different from zero, and thus the role of Antarctic surface mass balance in mitigating recent sea-level rise may be minor.

6. Conclusions

This study employs Polar MM5, a model optimized for use in polar regions, for the first time to evaluate recent precipitation trends over Antarctica. Two sets of simulations, each driven by a different reanalysis, yield similar spatial patterns of annual and seasonal precipitation trends over Antarctica. By comparing these two datasets with each other and with observations, the reanalyses used to drive them, and an independent reanalysis (JRA), the uncertainty can be estimated. The similarity between the trends for the two runs, as well as their agreement with observations, lends confidence that the results are robust. The PMM5_E40 hydrologic cycle is similar to that of its 'parent' reanalysis, E40, although it predicts about 40 mm yr^{-1} more annual precipitation over the GIS. The PMM5_NN2 hydrologic cycle appears to be an improvement over its 'parent' reanalysis, NN2, generally capturing mean precipitation, temporal changes and interannual variability with more skill compared to observations from ice cores and snow stakes. Both of the Polar MM5 runs simulate precipitation trends for 1985–2001 that are closer to zero than their respective reanalyses.

Our results indicate that there is a substantial amount of spatial and temporal variability in the Antarctic surface mass balance. The annual variability and trends over Antarctica are the small residual of larger seasonal variability and trends that appear to be related to recent climate change, particularly seasonally varying trends in the SAM. This complex topic will be addressed in a follow-on publication. Though considerable changes are happening regionally, averaged over Antarctica, the annual trend in Antarctic precipitation, which is important for sea-level change assessments, appears to be close to zero. Although this study is over a different time-period and employs different techniques, the model and observational results presented here do not support the significant upward accumulation trend suggested by Davis *et al.* (2005) for the 1992–2003 period over East Antarctica.

This research is funded by the National Science Foundation Office of Polar Programs Glaciology Program (Grant NSF-OPP-0337948). Sincere gratitude is owed to members of the International Transantarctic Science Expedition, who provided accumulation records from ice cores and related

assistance. Particular thanks are due to: Jiahong Wen, Ian Goodwin, Tas van Ommen, Vin Morgan, Hans Oerter, Ellen Mosley-Thompson, Victor Lagun, Steve Colwell, Susan Kaspari, Paul Mayewski, Elisabeth Isaksson, Robert Mulvaney and Massimo Frezzotti. We are grateful to Willem Jan van de Berg for helping resolve several issues with ERA-40 precipitation. The Japanese 25 year reanalysis, for which there is not a journal citation, was provided by the Japan Meteorological Agency and the Central Research Institute of Electric Power Industry (http://www.jreap.org). The ERA-40 data were obtained from the University Corporation for Atmospheric Research Data Support Section (http://www.dss.ucar.edu). The NCEP-DOE-II data were obtained from the National Oceanic and Atmospheric Institute's Climate Diagnostics Centre (http://www.cdc.noaa.gov).

References

Bromwich, D. H. 1988 Snowfall in high southern latitudes. *Rev. Geophys.* **26**, 149–168.

Bromwich, D. H. & Robasky, F. M. 1993 Recent precipitation trends over the polar ice sheets. *Meteor. Atmos. Phys.* **51**, 259–274. (doi:10.1007/BF01030498)

Bromwich, D. H. & Fogt, R. L. 2004 Strong trends in the skill of the ERA-40 and NCEP/NCAR Reanalyses in the high and middle latitudes of the Southern Hemisphere, 1958–2001. *J. Climate* **17**, 4603–4619. (doi:10.1175/3241.1)

Bromwich, D. H., Cassano, J. J., Klein, T., Heinemann, G., Hines, K. M., Steffen, K. & Box, J. E. 2001 Mesoscale modeling of katabatic winds over Greenland with the Polar MM5. *Mon. Wea. Rev.* **129**, 2290–2309. (doi:10.1175/1520-0493(2001)129<2290:MMOKWO>2.0.CO;2)

Bromwich, D. H., Guo, Z., Bai, L.-S. & Chen, Q.-S. 2004 Modeled Antarctic precipitation. Part I: spatial and temporal variability. *J. Climate* **17**, 427–447. (doi:10.1175/1520-0442(2004)017<0427:MAPPIS>2.0.CO;2)

Budd, W. F. & Simmonds, I. 1991 The impact of global warming on the Antarctic mass balance and global sea level. In *Proc. Int. Conf. on the role of the Polar regions in global change, vol. 1, University of Alaska Fairbanks, Alaska, 11–15 June 1990*, pp. 489–494.

Cassano, J. J., Box, J. E., Bromwich, D. H., Li, L. & Steffen, K. 2001 Verification of Polar MM5 simulations of Greenland's atmospheric circulation. *J. Geophys. Res.* **106**, 33 867–33 890. (doi:10.1029/2001JD900044)

Davis, C. H., Li, Y., McConnell, J. R., Frey, M. M. & Hanna, E. 2005 Snowfall-driven growth in east Antarctic Ice Sheet mitigates recent sea-level rise. *Science* **308**, 1898–1901. (doi:10.1126/science.1110662)

De la Mare, W. K. 1997 Abrupt mid-twentieth century decline in Antarctic sea-ice extent from whaling records. *Nature* **389**, 57–60. (doi:10.1038/37956)

Ekaykin, A. A., Lipenkov, V. Y., Kuzmina, I. N., Petit, J. R., Masson-Delmotte, V. & Johnsen, S. J. 2004 The changes in isotope composition and accumulation of snow at Vostok Station over the past 200 years. *Ann. Glaciol.* **39**, 569–575.

Fogt, R. L. & Bromwich, D. H. 2006 Decadal variability of the ENSO teleconnection to the high latitude South Pacific governed by coupling with the Southern Annular Mode. *J. Climate* **19**, 979–997.

Fiorino, M. 2004 A multi-decadal daily sea surface temperature and sea ice concentration data set for the ERA-40 reanalysis. ERA-40 Project Report Series No. 12. European Centre for Medium-Range Weather Forecasts. Reading, UK.

Frezzotti, M. *et al.* 2004 New estimations of precipitation and surface sublimation in East Antarctica from snow accumulation measurements. *Clim. Dyn.* **23**, 803–813. (doi:10.1007/s00382-004-0462-5)

Frezzotti, M. *et al.* 2005 Spatial and temporal variability of snow accumulation in East Antarctica from traverse data. *J. Glaciol.* **51**, 113–124.

Genthon, C. 2004 Space-time Antarctic surface mass balance variability from climate models. *Ann. Glaciol.* **39**, 271–275.

Genthon, C. & Krinner, G. 2001 Antarctic surface mass balance and systematic biases in general circulation models. *J. Geophys. Res.* **106**, 20 653–20 664. (doi:10.1029/2001JD900136)

Genthon, C., Kaspari, S. & Mayewski, P. A. 2005 Interannual variability of the surface mass balance of West Antarctica from ITASE cores and ERA-40 reanalyses, 1958–2000. *Clim. Dyn.* **24**, 759–770. (doi:10.1007/s00382-005-0019-2)

Giovinetto, M. B. & Bentley, C. R. 1985 Surface balance in ice drainage systems of Antarctica. *Antarct. J. US* **20**, 6–13.

Giovinetto, M. B. & Zwally, H. J. 2000 Spatial distribution of net surface accumulation on the Antarctic Ice Sheet. *Ann. Glaciol.* **31**, 171–178.

Goodwin, I. D., Higham, M., Allison, I. & Ren, J. 1994 Accumulation variability in eastern Kemp land, Antarctica. *Ann. Glaciol.* **20**, 202–206.

Grell, G. L., Dudhia, J. & Stauffer, D. R. 1994 A description of the fifth-generation Penn State/NCAR mesoscale model (MM5). *NCAR Tech. Note NCAR/TN-398+STR*, p. 117. Boulder, USA: National Center for Atmospheric Research.

Guo, Z., Bromwich, D. H. & Cassano, J. J. 2003 Evaluation of Polar MM5 simulations of Antarctic atmospheric circulation. *Mon. Wea. Rev.* **131**, 384–411. (doi:10.1175/1520-0493(2003)131<0384:EOPMSO>2.0.CO;2)

Guo, Z., Bromwich, D. H. & Hines, K. M. 2004 Modeled Antarctic precipitation. Part II: ENSO signal over West Antarctica. *J. Climate* **17**, 448–465. (doi:10.1175/1520-0442(2004)017<0448:MAPPIE>2.0.CO;2)

Higham, M. & Craven, M. 1997 Surface mass balance and snow surface properties from the Lambert Glacier basin traverses 1990–94. *Antarctic CRC Research Report 9*, p. 129. Hobart, Tasmania: Cooperative Research Centre for the Antarctic and Southern Ocean Environment.

Hines, K. M., Grumbine, R. W., Bromwich, D. H. & Cullather, R. I. 1999 Surface energy balance of the NCEP MRF and NCEP–NCAR reanalysis in Antarctic latitudes during FROST. *Wea. Forecasting* **14**, 851–866. (doi:10.1175/1520-0434(1999)014<0851:SEBOTN>2.0.CO;2)

Hines, K. M., Bromwich, D. H. & Marshall, G. J. 2000 Artificial surface pressure trends in the NCEP/NCAR reanalysis over the Southern Ocean and Antarctica. *J. Climate* **13**, 3940–3952. (doi:10.1175/1520-0442(2000)013<3940:ASPTIT>2.0.CO;2)

Kaspari, S., Mayewski, P. A., Dixon, D. A., Spikes, V. B., Sneed, S. B., Handley, M. J. & Hamilton, G. S. 2004 Climate variability in West Antarctica derived from annual accumulation rate records from ITASE firn/ice cores. *Ann. Glaciol.* **39**, 585–594.

Kalnay, E. *et al.* 1996 The NCEP/NCAR 40-year reanalysis project. *Bull. Am. Meteorol. Soc.* **77**, 437–471. (doi:10.1175/1520-0477(1996)077<0437:TNYRP>2.0.CO;2)

Kanamitsu, M., Ebisuzaki, W., Woolen, J., Potter, J. & Fiorino, M. 2002 NCEP/DOE AMIP-II reanalysis (R-2). *Bull. Am. Met. Soc.* **83**, 1631–1643. (doi:10.1175/BAMS-83-11-1631(2002)083<1631:NAR>2.3.CO;2)

Kistler, R. *et al.* 2001 The NCEP/NCAR 50-year Reanalysis: monthly means CDROM and documentation. *Bull. Am. Met. Soc.* **82**, 247–267. (doi:10.1175/1520-0477(2001)082<0247:TNNYRM>2.3.CO;2)

Liston, G. E. & Winther, J.-G. 2005 Antarctic surface and subsurface snow and ice melt fluxes. *J. Climate* **18**, 1469–1481. (doi:10.1175/JCLI3344.1)

Liu, H., Jezek, K., Li, B. & Zhao, Z. 2001 *Radarsat Antarctic mapping project digital elevation model version 2*. Boulder, USA: National Snow and Ice Data Center. Digital media.

Leuliette, E. R., Nerem & Mitchum, G. 2004 Calibration of TOPEX/Poseidon and Jason altimeter data to construct a continuous record of mean sea level change. *Mar. Geod.* **27**, 79–94. (doi:10.1080/01490410490465193)

Magand, O., Frezzotti, M., Pourchet, M., Stenni, B., Genoni, L. & Fily, M. 2004 Climate variability along latitudinal and longitudinal transects in East Antarctica. *Ann. Glaciol.* **39**, 351–358.

Marshall, G. J. 2003 Trends in the Southern Annular Mode from observations and reanalyses. *J. Climate* **16**, 4134–4143. (doi:10.1175/1520-0442(2003)016<4134:TITSAM>2.0.CO;2)

Marshall, G. J. & Harangozo, S. A. 2000 An appraisal of NCEP/NCAR reanalysis MSLP data viability for climate studies in the South Pacific. *Geophys. Res. Lett.* **27**, 3057–3060. (doi:10.1029/2000GL011363)

Marshall, G. J., Stott, P., Turner, J., Connolley, W. M., King, J. C. & Lachlan-Cope, T. A. 2004 Causes of exceptional atmospheric circulation changes in the Southern Hemisphere. *Geophys. Res. Lett.* **31**, L14 205. (doi:10.1029/2004GL019952)

Meyerson, E. A., Mayewski, P. A., Whitlow, S. I., Meeker, L. D., Kreutz, K. J. & Twickler, M. S. 2003 The extratropical expression of ENSO recorded in a South Pole glaciochemical time series. *Ann. Glaciol.* **35**, 430–436.

Mosley-Thompson, E., Paskievitch, J. F., Gow, A. J. & Thompson, L. G. 1999 Late 20th Century increase in South Pole snow accumulation. *J. Geophys. Res.* **104**, 3877–3886. (doi:10.1029/1998JD200092)

Nereson, N. A., Waddington, E. D., Raymond, C. F. & Jacobsen, H. P. 1996 Predicted age-depth scales for Siple Dome and inland WAIS ice cores in West Antarctica. *Geophys. Res. Lett.* **23**, 3163–3166. (doi:10.1029/96GL03101)

Oerter, H., Wilhelms, F., Jung-Rothenhäusler, F., Göktas, F., Miller, H., Graf, W. & Sommer, S. 2000 Accumulation rates in Dronning Maud Land, Antarctica, as revealed by dielectric-profiling measurements of shallow firn cores. *Ann. Glaciol.* **30**, 27–34.

Ohmura, A., Wild, M. A. & Bengtsson, L. 1996 A possible change in mass balance of Greenland and Antarctic Ice Sheets in the coming century. *J. Climate* **9**, 2124–2135. (doi:10.1175/1520-0442(1996)009<2124:APCIMB>2.0.CO;2)

Rignot, E. & Thomas, R. H. 2002 Mass balance of polar ice sheets. *Science* **297**, 1502–1506. (doi:10.1126/science.1073888)

Simmons, A. J., Jones, P. D., da Costa Bechtold, V., Beljaars, A. C. M., Kallberg, P. W., Saarinen, S., Uppala, S. M., Viterbo, P. & Wedi, N. 2004 Comparison of trends and low-frequency variability in CRU, ERA-40, and NCEP/NCAR analyses of surface air temperature. *J. Geophys. Res.* **109**, D24 115. (doi:10.1029/2004JD005306)

Thomas, R. *et al.* 2004 Accelerated seal-level rise from West Antarctica. *Science* **306**, 255–258. (doi:10.1126/science.1099650)

Thompson, D. W. J. & Wallace, J. M. 2000 Annular modes in the extratropical circulation. Part I: Month-to-month variability. *J. Climate* **13**, 1000–1016. (doi:10.1175/1520-0442(2000)013<1000:AMITEC>2.0.CO;2)

Turner, J., Connolley, W. M., Leonard, S., Marshall, G. J. & Vaughan, D. G. 1999 Spatial and temporal variability of net snow accumulation over the Antarctic from ECMWF re-analysis project data. *Int. J. Climatol.* **19**, 697–724. (doi:10.1002/(SICI)1097-0088(19990615)19:7<697::AID-JOC392>3.0.CO;2-3)

Turner, J., Lachlan-Cope, T. A., Colwell, S. & Marshall, G. J. In press. A positive trend in western Antarctic Peninsula precipitation over the last 50 years reflecting regional and Antarctic-wide atmospheric circulation changes. *Ann. Glaciol.* **41**.

Uppala, S. M. *et al.* 2005 The ERA-40 Reanalysis. *Q. J. R. Meteorol. Soc.* **131**, 2961. (doi:10.1256/qj.04.176)

Van de Berg, W. J., van den Broeke, M. R., Reijmer C. H. & van Meijgaard, E. In press *a*. Characteristics of the Antarctic surface mass balance (1958–2002) using a regional atmospheric climate model. *Ann. Glaciol.* **41**.

Van de Berg, W. J., van den Broeke, M. R., Reijmer C. H. & van Meijgaard, E. In press *b*. Reassessment of the Antarctic surface mass balance using calibrated output of a regional atmospheric climate model. *J. Geophys. Res.*

Van Lipzig, N. P. M., van Meijgaard, E. & Oerlemans, J. 2002 The spatial and temporal variability of the surface mass balance in Antarctica: results from a regional atmospheric climate model. *Int. J. Climatol.* **22**, 1197–1217. (doi:10.1002/joc.798)

Vaughan, D. G. 2005 How does the Antarctic Ice Sheet affect sea level rise? *Science* **308**, 1877–1878. (doi:10.1126/science.1114670)

Vaughan, D. G., Bamber, J. L., Giovinetto, M., Russell, J. & Cooper, A. P. R. 1999 Reassessment of net surface mass balance in Antarctica. *J. Climate* **12**, 933–946. (doi:10.1175/1520-0442(1999)012<0933:RONSMB>2.0.CO;2)

Wen, J., Kang, J., Wang, D., Bo, S., Yuanshan, L., Zhongqin, L. & Jun, L. 2001 Density, stratigraphy and accumulation at DT001 in Princess Elizabeth Land, East Antarctic Ice Sheet. *Polar Meteorol. Glaciol.* **15**, 43–54.

Xiao, C., Ren, J., Dahe, Q., Hongqin, L., Weizhen, S. & Allison, I. 2001 Complexity of the climatic regime over the Lambert Glacier basin of the East Antarctica ice sheet: firn core evidences. *J. Glaciol.* **47**, 160–162.

Xie, P. P. & Arkin, P. A. 1998 Global monthly precipitation estimates from satellite-observed outgoing longwave radiation. *J. Climate* **11**, 137–164. (doi:10.1175/1520-0442(1998)011<0137:GMPEFS>2.0.CO;2)